KNIGHT CANCER Institute
OHSU

Brian J. Druker, M.D.
Director, Knight Cancer Institute
Associate Dean for Oncology, School of Medicine
JELD-WEN Chair of Leukemia Research

tel   503 494-5596
fax   503 494-3688

drukerb@ohsu.edu
www.ohsu.edu

Mail Code: KR-HEM
3181 S.W. Sam Jackson Park Rd.
Portland, OR 97239

August 25, 2022

Dear Tang Prize Foundation Committee,

I am writing to express my sincere gratitude for your generous support of my research program. My current research strives to improve the outcome of therapy for patients with leukemia by translating the knowledge of the molecular pathogenesis of cancer into specific therapies. Our progress report detailing what we have accomplished with your funding is attached. As you will see, we have generated significant new insights into how the order of acquisition of mutations associated with leukemia impacts the disease phenotype. These insights have led us to propose new treatment strategies that are moving into clinical trials. I'm incredibly grateful for the Tang Prize Foundation's support of this work.

Thank you for your steadfast commitment to biopharmaceutical science.

Sincerely,

Brian J. Druker, M.D.

Epigenetics of Mutation-Order-Dependent Phenotypes in Myeloid Leukemia
Brian J. Druker, MD
Tang Prize—Outcomes Report

Background
Cancer is frequently described as the sum of the properties of individual driver mutations. Vogelstein famously stated that "accumulation, rather than order, is most important." However, mutation order is not random. In acute myeloid leukemia (AML), mutations commonly co-occur as a paring of a differentiation blocking mutation (i.e., AML-ETO, CBFβ-SMMHC, CEBPA) and a proliferative driver (i.e., FLT3-ITD, NRAS, CSF3R). The former can be identified prior to overt disease development, while the later cannot. Thus, it is widely believed that differentiation blockade occurs early while proliferative drivers arise late in AML development. However, there is no mechanistic explanation for this finding. Using mutations in colony stimulating factor 3 receptor (CSF3R) and CCAAT enhancer binding protein alpha (CEBPA) as representatives of these distinct functional classes, my team demonstrated that the order in which these mutations are introduced dramatically alters the leukemic phenotype.

CEBPA directs the establishment of normal lineage-specific enhancers during myeloid development. Mutations in CEBPA occur in 10% of AML and disrupt DNA binding. CEBPA mutations frequently co-occur with activating mutations in CSF3R. In isolation, mutations in CSF3R drive a myeloproliferative neoplasm through constitutive JAK/STAT signaling. Using an inducible retroviral system, we showed that when CEBPA mutations are introduced first, myeloid differentiation is blocked, allowing leukemia to develop. In contrast, CEBPA mutations introduced after mutant CSF3R cannot block differentiation, and an acute leukemia does not develop. This is the first demonstration that mutation order exerts cell-intrinsic impacts on leukemia development. Understanding the biology of these mutation-ordered phenotypes was the major focus of this work.

Experimental Aims
Aim 1. Define the epigenetic consequences of mutation order

Aim 2. Establish the Role of LSD1 as a Regulator of The Enhancer Landscape in CEBPA mutant AML

Aim 3. Enhancer reactivation as a therapeutic strategy in CBF/CEBPA AML

Significance and Results

Acute Myeloid Leukemia
Acute Myeloid Leukemia (AML) is a deadly hematologic malignancy characterized by the accumulation of immature myeloblasts in the bone marrow and peripheral blood. The vast majority of patients are treated with cytarabine-based chemotherapy, an approach that remains unchanged for the last 40 years[1]. Although intensive research has brought about several novel, molecularly-guided treatments, these are rarely curative. For adults with AML, five-year survival is approximately 25%[2]. Therefore, new treatments guided by a deeper understanding of disease biology are needed.

Mutations in AML Occur in a Specific Order
Leukemia—like all cancers—results from the stepwise accumulation of mutations. When Fearon and Vogelstein first introduced their genetic model of colon tumorigenesis, they noted that while mutations often occur in a particular order, it is the total accumulation of mutations rather than
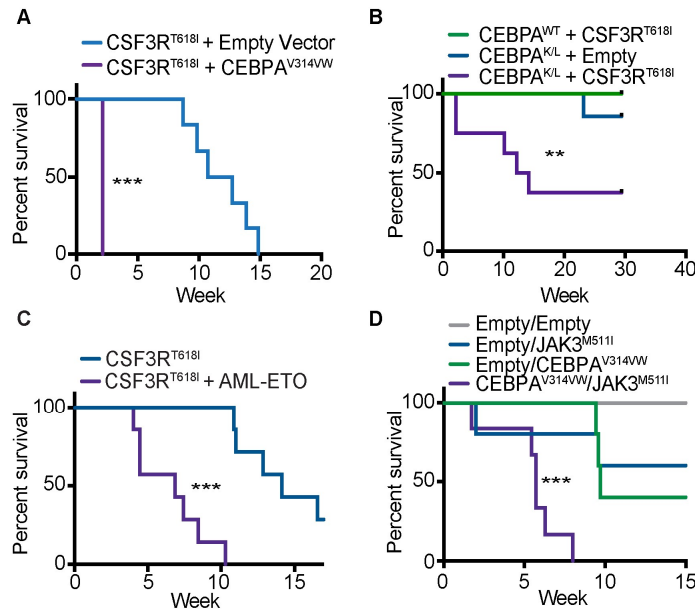
Figure 1. CEBPA and CSF3R Combine to Produce A Rapidly Lethal Myeloid Leukemia. Survival of mice transplanted with **A.** bone marrow cells retrovirally transduced with $CSF3R^{T618I}$ or the combination of $CSF3R^{T618I}$ and $CEBPA^{V314VW}$, **B.** fetal liver cells from wild type ($CEBPA^{WT}$) or harboring biallelic CEBPA mutations ($CEBPA^{K/L}$) transduced with empty vector or $CSF3R^{T618I}$, **C.** bone marrow cells transduced with $CSF3R^{T618I}$ or $CSF3R^{T618I}$+AML-ETO, **D.** bone marrow cells transduced empty vector, $JAK3^{M511I}$, $CEBPA^{V314VW}$ or the combination. **=$p<0.01$, ***=$p<0.001$ by log rank test.

their order that is most important[3]. Since that time, cancer is often described and modeled as the sum of the properties of individual driver mutations. **However, this summative model fails to account for the impact an early mutation may have on the manifestation of subsequent mutations**. Indeed, recent data has begun to challenge this principle. In the myeloid malignancies, there is increasing evidence that mutations of distinct functional classes occur at specific phases of leukemia development. The earliest events are mutations in global modifiers of the epigenome (i.e., DNMT3a and TET2), which often occur years to decades prior to leukemia development. Point mutations or fusion events involving lineage-determining transcription factors block myeloid differentiation and also occur early in disease development, though likely not as early as mutations in epigenetic modifiers[4]. Mutations that activate signaling pathways occur late in disease evolution. Mimicking extrinsic growth factor signaling, these mutations frequently cause myeloproliferation when present in isolation, but result in AML when combined with mutations from the other two classes.

Mutations in CEBPA Must Occur Prior to Mutations in CSF3R for Leukemia Initiation

The transcription factor CCAAT enhancer binding protein alpha (CEBPA) is a crucial determinant of myeloid lineage differentiation in normal hematopoiesis. CEBPA is mutated in approximately 10% of adult AML (represented here by $CEBPA^{V314VW}$) and 5% of pediatric AML, where it most frequently co-occurs with mutations in the colony stimulating factor 3 receptor (CSF3R)[5–8]. The receptor for granulocyte colony stimulating factor, CSF3R directs myeloid differentiation through downstream JAK/STAT signaling. Mutant CSF3R (represented here by $CSF3R^{T618I}$) results in ligand-independent signaling and in isolation produces a myeloproliferative neoplasm in isolation[9]. Mutant CSF3R and CEBPA combine to produce a rapidly lethal murine leukemia when
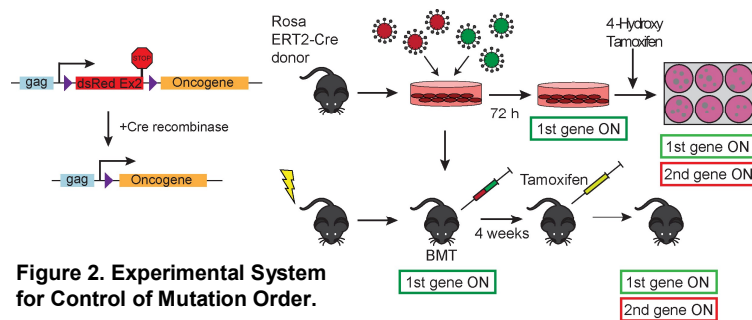
Figure 2. Experimental System for Control of Mutation Order.

introduced through retroviral bone marrow transplantation (Fig. 1A). Similar findings are seen when mutant CSF3R is introduced into fetal liver cells harboring endogenous CEBPA mutations or when CEBPA expression is suppressed via expression of the AML-ETO fusion protein (Fig. 1A, B). JAK/STAT activation through direct mutation ($JAK3^{M511I}$) can also initiate leukemia in combination with mutant CEBPA (Fig. 1D). As the timing of CEBPA mutations during AML evolution was unknown, we developed a retroviral system in which the induction of oncogene expression can be controlled temporally through
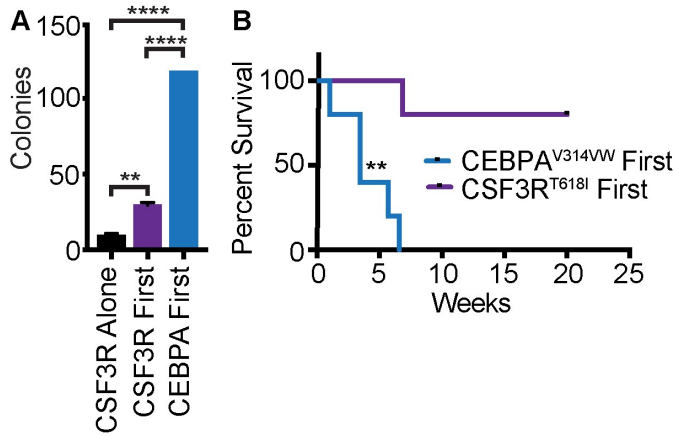
Figure 3. Mutation Order is an Important Determinant of Disease Phenotype. **A**. Colony assay from different mutation orders. ***=p<0.001, ****=p<0.0001 by ANOVA. **B.** Survival of mice transplanted with cells harboring different oncogene orders and treated with 4-OHT at week 4. **=p<0.01 by log-rank test.

tamoxifen-inducible Cre-mediated recombination (Fig. 2). When mutant CEBPA is expressed prior to mutant CSF3R, cytokine-independent colony formation is markedly enhanced (Fig. 3A). In contrast, when mutant CSF3R is expressed first, colony output is only modestly increased. These results are mirrored *in vivo* when recombination is induced 4 weeks after transplant. Mice receiving cells expressing mutant CEBPA first developed AML, while mice transplanted with CSF3R first cells developed AML with either markedly delayed kinetics (one mouse only) or no disease at all (Fig. 3B). **This is the first demonstration that the order in which mutations are introduced profoundly impacts disease phenotype and progression in AML. The importance of order of acquisition for other mutational pairings will be explored in Aim 1.**

Mutant CEBPA Disrupts Differentiation-Associated Enhancers

During normal myeloid development, CEBPA cooperates with the transcription factor PU.1 to establish the enhancer repertoire associated with myeloid differentiation[10,11]. My RNA-seq analysis of bone marrow expressing CSF3R[T618I] reveals activation of the CEBPA network and increased myeloid differentiation (Fig. 4A). Co-expression of CEBPA[V314VW] inhibits the CEBPA network and blocks myeloid differentiation. Transcription factor motif enrichment revealed putative STAT and IRF binding sites at the promoters of differentially expressed genes but did not reveal enrichment of CEBPA binding sites (Fig. 4B). To determine if CEBPA-dependent enhancers are responsible for the observed differentiation blockade, we performed chromatin immunoprecipitation followed by sequencing (ChIP-seq) in HoxB8- ER cells transduced with
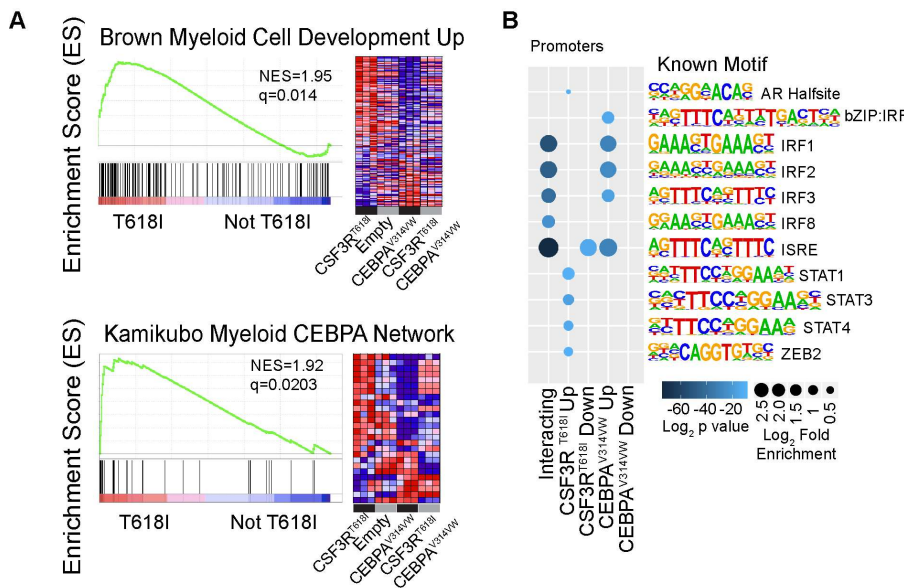
Figure 4. Mutant CEBPA blocks myeloid differentiation through disruption of wild type CEBPA binding to non-promoter elements. RNA-seq performed on mouse bone marrow transduced with empty vector, CSF3R[T618I], CEBPA[V314VW] or the combination. **A.** Gene set enrichment analysis. **B.** Transcription factor motif enrichment.

either oncogene in isolation or both CEBPA^{V314VW} and CSF3R^{T618I} in combination. HoxB8-ER cells are immortalized through expression of the HoxB8 gene fused to the estrogen receptor resulting in maintenance of a phenotype similar to the granulocyte-macrophage progenitor (GMP)[12]. Upon estrogen withdrawal, cells terminally differentiate into neutrophils. This differentiation is accelerated when CSF3R^{T618I} is expressed, and blocked when CEBPA^{V314VW} is co-expressed (Fig. 5A). ChIP-seq analysis revealed that CSF3R^{T618I} activates enhancers associated with differentiation in a CEBPA-dependent manner (Example differentiation-associated enhancer, Fig. 5B). Co expression of CEBPA^{V314VW} blocks activation of these enhancers, preventing differentiation. **Since enhancer activation precedes promoter activation, this provides a plausible mechanism for the impact of mutation order on disease phenotype**[13].
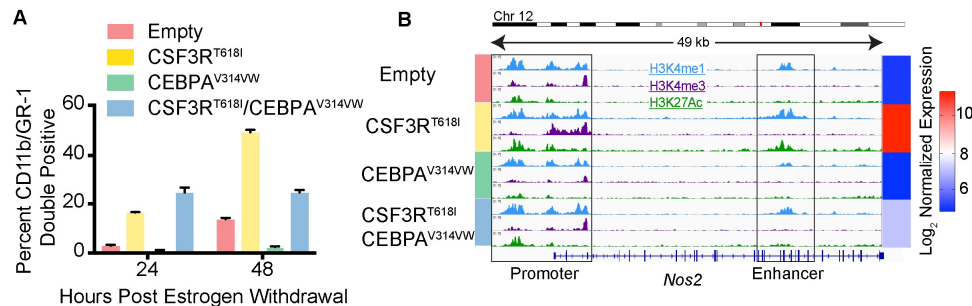
Figure 5. Mutant CEBPA disrupts myeloid differentiation through disruption of myeloid lineage enhancers. ChIP-seq for histone marks was performed on HoxB8-ER cells harboring empty vector, CSF3R^{T618I}, CEBPA^{V314VW} or the combination. **A.** Expression of CD11b and GR1 assessed by flow cytometry. **B.** Example enhancer at Nos2 locus.

These findings were published in: Braun TP, Okhovat M, Coblentz C, Carratt SA, Foley A, Schonrock Z, Curtiss BM, Nevonen K, Davis B, Garcia B, LaTocha D, Weeder BR, Grzadkowski MR, Estabrook JC, Manning HG, Watanabe-Smith K, Jeng S, Smith JL, Leonti AR, Ries RE, McWeeney S, Di Genua C, Drissen R, Nerlov C, Meshinchi S, Carbone L, Druker BJ, Maxson JE, (2019). Myeloid lineage enhancers drive oncogene synergy in CEBPA/CSF3R mutant acute myeloid leukemia. Nature Communications, Nov 29;10(1):5455. PubMed PMID: 31784538

Enhancer Reactivation as a Therapeutic Strategy in CEBPA Mutant AML

There is increasing interest in the targeting of epigenetic modifiers as a therapeutic strategy in AML[14]. However, these studies have been limited to specific genetic subtypes of AML (i.e., MLL rearranged, or DNMT3a mutant). We performed drug screening using a panel of 150 inhibitors on a CEBPA/CSF3R mutant AML cell line derived from murine bone marrow, which revealed sensitivity to inhibition of lysine demethylase 1 (LSD1, Fig. 6A). LSD1 is responsible for the decommissioning of enhancers through removal of H3K4me1/2 marks[15]. This screen also revealed sensitivity to JAK/STAT inhibition, consistent with the known signaling downstream of CSF3R. Covalent (GSK2879552 and GSK-LSD1) inhibitors of LSD1 reversed the differentiation blockade induced by mutant CEBPA (Fig. 6B). In mice harboring CEBPA/CSF3R mutant AML however, neither LSD1 nor JAK/STAT inhibition (ruxolitinib) improved survival (Fig. 6C, D). However, in combination, LSD1 and JAK/STAT inhibition controlled peripheral blast counts and doubled median survival. (Fig. 6E, F).

These findings were published in: Braun TP, Coblentz C, Curtiss BM, Schonrock Z, Carratt SA, Maniaci B, Druker BJ, Maxson JE, (2020). Combined inhibition of JAK/STAT pathway and lysine-specific demethylase 1 as a therapeutic strategy in CSF3R/CEBPA mutant acute myeloid leukemia, PNAS. June 16; 117(24):13670-13679. PMID: 32471953.

Dual Targeting of KIT and LSD1 in KIT-mutant AML

We also evaluated whether combined inhibition of KIT and LSD1 might demonstrate similar effects in KIT mutant AML. In AML cell lines, we found strong drug synergy between the KIT inhibitor avapritinib and LSD1 inhibition (Fig. 7). We performed a comprehensive transcriptional and epigenetic analysis which implicated MYC and PU.1 as key regulatory transcription factors driving the drug response (Figs. 8-9). We validated these findings in primary KIT-mutant AML samples and found similar efficacy to that which we observed in cell lines (Fig. 10). Collectively, these data provide pre-clinical proof of concept for dual kinase plus LSD1 inhibition in KIT-mutant AML.
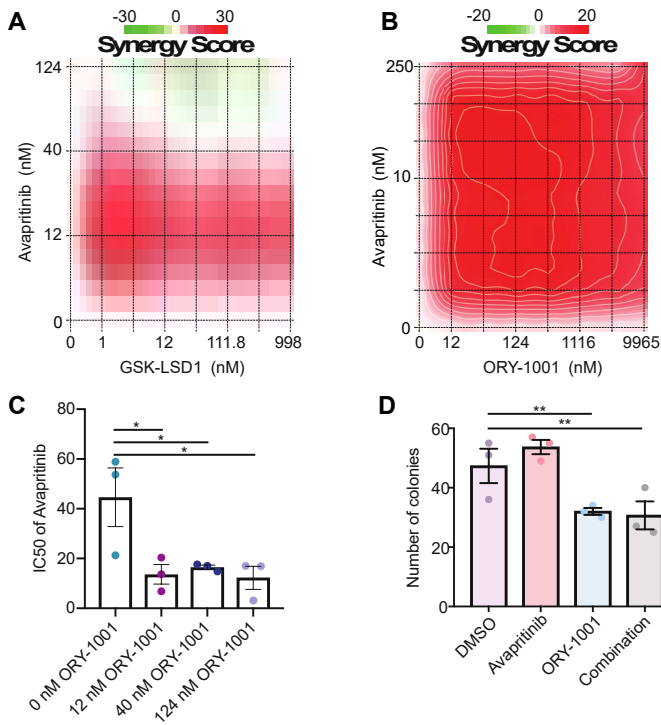
Figure 6. Combined inhibition of LSD1 and JAK/STAT improves survival in CEBPA/CSF3R mutant murine AML. A. High throughput drug screen on CEBPA/CSF3R mutant murine AML cells. Percentage of median IC50 of all prior samples screened is displayed. **B.** Morphologic differentiation after LSD1 inhibitor treatment (4 nM) for 48h. **C.** Survival of mice treated with ruxolitinib or GSK2879552 (90 mg/kg/day or 1.5 mg/kg/day given in twice daily divided dose). **D.** WBC counts from mice in C. **E.** Survival of mice treated with the combination of ruxolitinib and GSK2879552. **F.** WBC counts for mice in E.
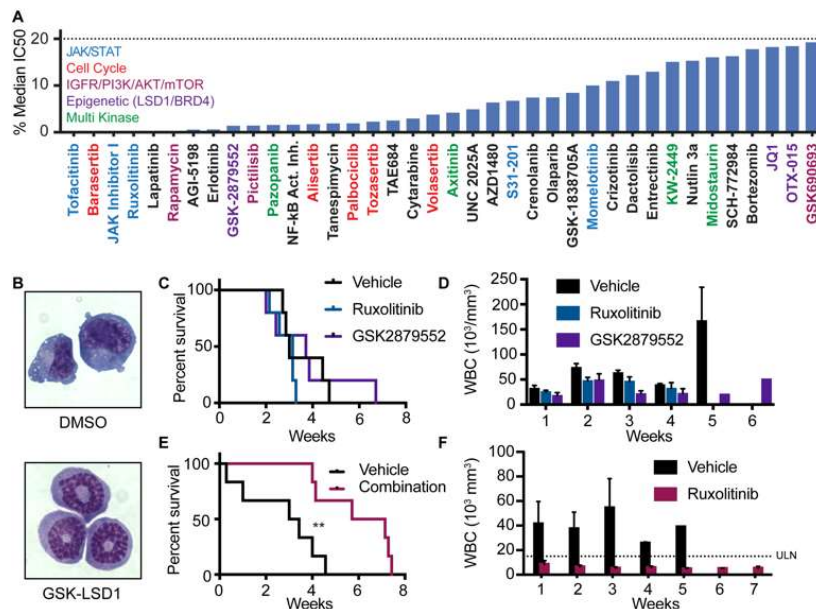
Figure 7. Synergistic cytotoxicity of dual KIT and LSD1 inhibition in KIT mutant AML cell line. A. and B. Drug matrix of Kasumi-1 cells treated for 72 h with avapritinib and GSK-LDS1 (A) or ORY-1001 (B) with synergy assessed by zero interaction potency (ZIP) score. **C.** IC50 of avapritinib with different concentrations of ORY-1001 in Kasumi-1 cells treated for 72 h; one-way ANOVA with Holm-Sidak correction. **D.** Colony assay using healthy CD34+ cells in human methocult with cytokines, treated for 14 days with avapritinib (12 nM) and/or ORY-1001 (12 nM); two-way ANOVA.
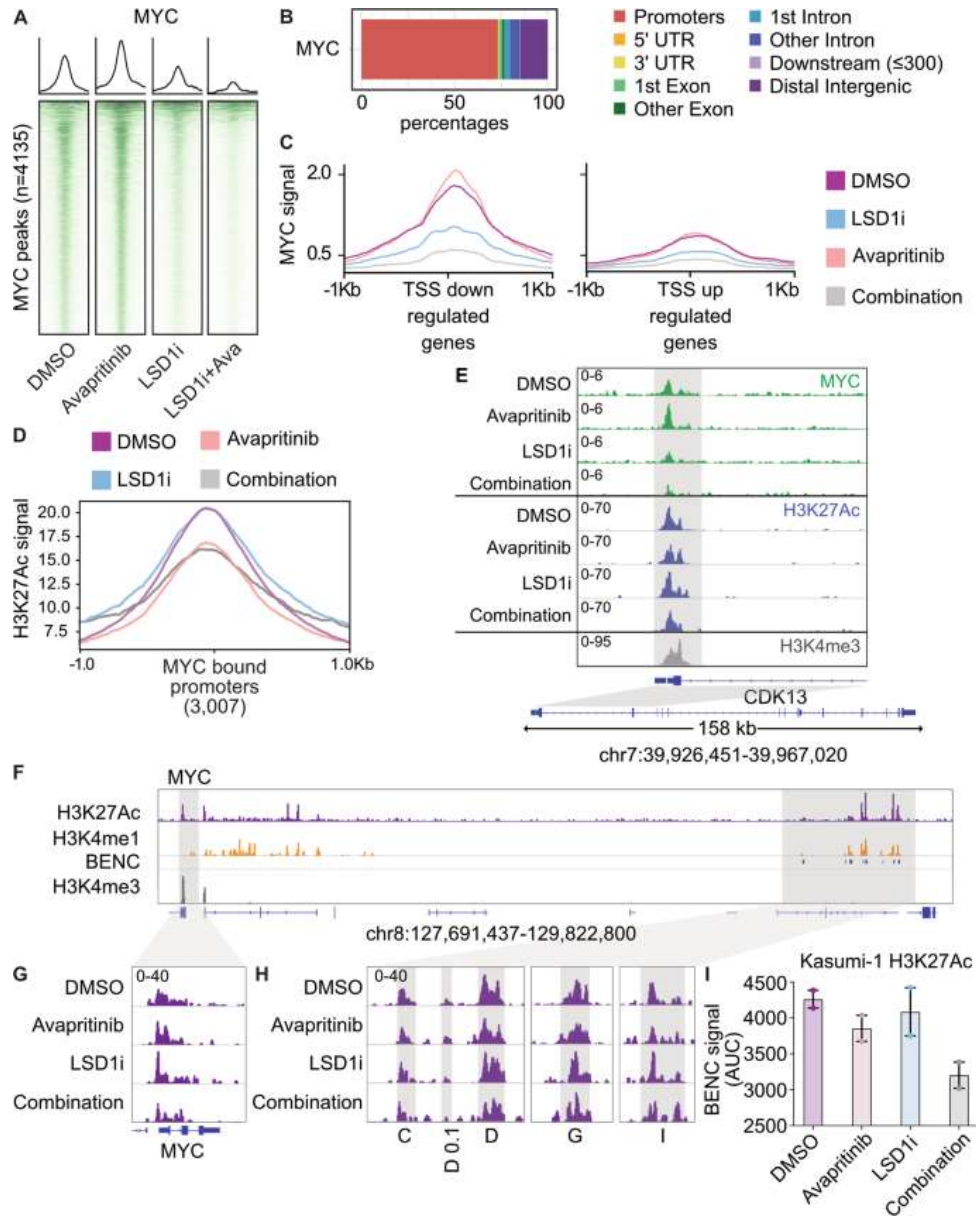
Figure 8. Repression of MYC bound promoters of cell cycle related programs. A. Kasumi-1 cells were treated for 24 h with avapritinib (12 nM) and/or GSK-LSD1 (12 nM; LSD1i) then subject to CUT&RUN (*n* = 2/group). Heatmaps of global signal for MYC at high confidence consensus peaks (peak apex ± 1 kb). **B.** Annotation of consensus MYC peaks. **C.** MYC signal at TSSs of down or up regulated genes defined by RNA-seq. **D.** H3K27Ac signal at all MYC bound promoters in Kasumi-1 cells after 24 h of treatment with avapritinib (12 nM) and/or GSK-LSD1 (12 nM; LSD1i). **E.** Gene ontology term enrichment for MYC bound promoters. **F.** Histone mark visualization with Integrative Genomics Viewer (IGV) at the MYC and blood enhancer cluster (BENC) locus (*n* = 2/group). BENC modules were identified with Kasumi-1 H3K4me1 signal that overlaps with the previously published modules [24]. **G** Histone acetylation in Kasumi-1 cells at the *MYC* locus. **H** Histone acetylation at active BENC modules. Active BENC modules were defined by presence of H3K27Ac signal. Modules without acetylation were excluded. **I** AUC of acetylation signal at active BENC modules.
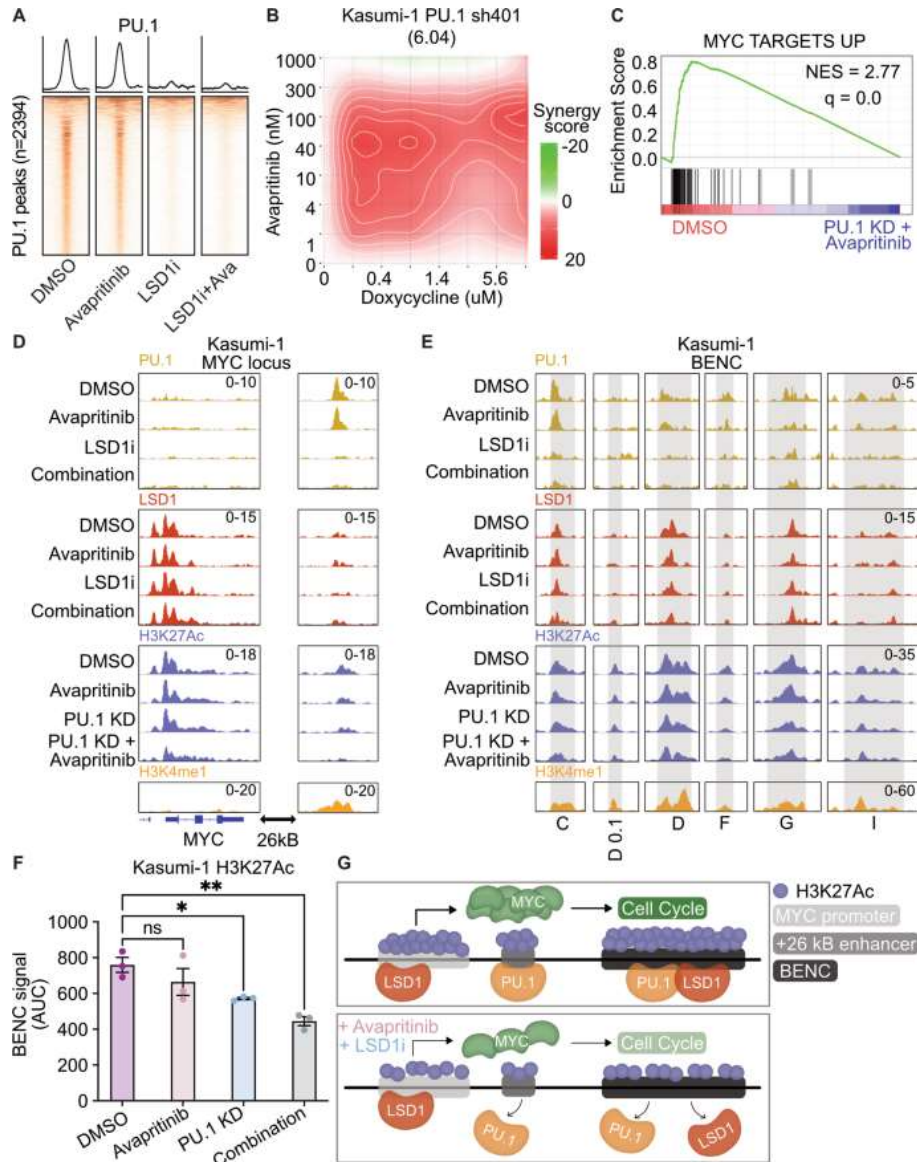
Figure 9. Loss of PU.1 binding at MYC enhancer resulting in loss of MYC enhancer and promoter activation. A. Kasumi cells treated for 24 h with avapritinib (12 nM) and/or GSK-LSD1 (12 nM; LSD1i) then subject to CUT&RUN for PU.1 (*n* = 2/group). Heatmaps of global signal for PU.1 at high confidence consensus PU.1 peaks (peak apex ± 1 kb). **B.** Drug matrix of avapritinib and doxycycline on Kasumi-1 PU.1 sh401 cells treated for 72 h. Synergy assessed by ZIP scores. ZIP score reported in parentheses. **C.** Depleted gene sets from bulk RNA-seq on PU.1 sh401, induced with doxycycline (1 μg/mL) 48 h before treatment with avapritinib (50 nM) for 24 h. NES normalized enrichment score (*q* < 0.05). GSEA *p* value calculated by empirical permutation test and FDR adjusted. **D., E.**. Kasumi-1 cells treated for 24 h with avapritinib (50 nM) and/or doxycycline (1 μg/mL) to induce PU.1 knockdown were used to perform CUT&Tag for H3K27Ac (*n* = 3/group). H3K4me1, PU.1, and LSD1 signal from above datasets in Kasumi-1 cells. Visualization of +26 Kb MYC and active modules of the blood super-enhancer cluster (BENC). BENC modules are defined Kasumi-1 H3K4me1 signal that intersects with the previously published coordinates for the BENC [24]. The presence of H3K27Ac signal was used to define active modules. **F.** Quantification of cumulative AUC of H3K27Ac signal at active BENC modules; one-way ANOVA with Holms-Sidak correction. Error bars representing SEM. **p* < 0.05, ***p* < 0.01. **G.** Model describing loss of PU.1 binding after dual LSD1 and KIT inhibition at *MYC* + 26 kB enhancer and BENC. PU.1 no longer activates *MYC* promoter resulting in decreased MYC protein, leading to decreased expression of MYC target genes including those involved with cell proliferation.
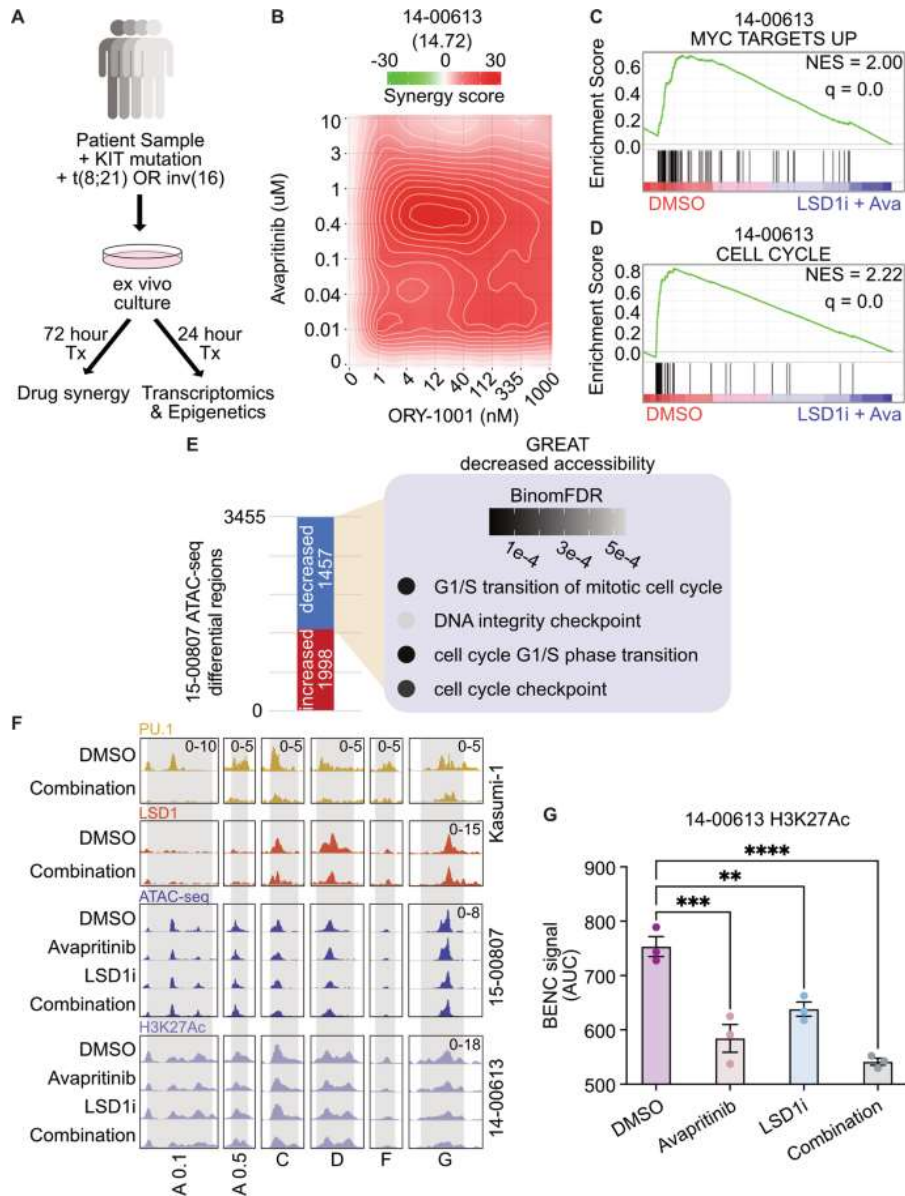
Figure 10. KIT and LSD1 inhibition synergistically target *KIT*-mutant AML patient samples resulting in decreased MYC and cell cycle programs. A. Experimental strategy for *KIT*-mutant patient samples. Frozen viable samples were cultured ex vivo and treated for 24 h before bulk RNA-seq and ATAC-seq. For synergy analysis, samples were drug treated for 72 h before assessing drug synergy. **B.** Drug matrix of patient sample 14-00613 treated for 72 h with avapritinib and ORY-1001 with synergy assessed by ZIP score. ZIP score reported in parentheses. **C., D.** Select depleted gene sets from bulk RNA-seq on 14-00613 treated with avapritinib (50 nM) and ORY-1001 (12 nM) or DMSO for 24 h. NES normalized enrichment score ($q < 0.05$). GSEA p value calculated by empirical permutation test and FDR adjusted. **E.** Differential analysis of bulk ATAC-seq on 15-00807 treated with avapritinib (50 nM) and ORY-1001 (50 nM) compared to DMSO. Enrichment of GO terms for regions with significantly decreased accessibility. **F.** Visualization of Kasumi-1 PU.1 and LSD1 from above datasets, 15-00807 bulk ATAC-seq, and 14-00613 H3K27Ac at active BENC modules [24] ($n = 3$/group). BENC modules defined by previously identified loci that overlap with H3K4me1 signal in Kasumi-1 cells. Active modules were designated based on presence of H3K27Ac signal. H3K27Ac CUT&Tag was performed on 14-00613 following 24 hr treatment with avapritinib (350 nM) and/or ORY-1001 (12 nM). **G.** Quantification of 14-00613 H3K27Ac signal at active BENC modules by comparing AUC; one-way ANOVA with Holm-Sidak correction. Error bars representing SEM. **$p < 0.01$, *** $p < 0.001$, ****$p < 0.0001$.

The findings in this section, *Dual Targeting of KIT and LSD1 in KIT-mutant AML* (Figs. 6-10), were published in: Curtiss BM, VanCampen J, Kong GL, Yashar W, Tsang YH, Horton W, Coleman DJ, Estabrook J, Lusardi TA, Mills GB, Druker BJ, Maxson JE, Braun TP, (2022). PU.1 and MYC transcriptional network defines synergistic drug responses to KIT and LSD1 inhibition in acute myeloid leukemia. Leukemia Jul;36(7):1781-1793.